Short Communication

Corrosion and Aging Behavior of Epoxy/Polyurethane Coatings on Carbon Steel in a Subhumid Environment

Jialiang Song, Xuan Liu, Wei Hu, Taiyang Zhu, Kui Xiao[*] and Jin Gao[*]

Corrosion and Protection Center, University of Science and Technology Beijing, Beijing 100083, China.
[*]E-mail: xiaokui@ustb.edu.cn

To study the corrosion and aging characteristics of a carbon steel coating system in a subhumid atmosphere of the northern temperate zone, Beijing and Zhengzhou were selected to conduct outdoor exposure tests on the carbon steel coating system. The coating system was tested by electrochemical impedance spectroscopy, and Q345 bare metal material was tested by a polarization curve. According to the curve fitting analysis obtained from the tests, the results show that the coating system has a good protective effect on the substrate within one year, and the decrease in the low-frequency impedance modulus also indicates the aging trend of the coating surface. The corrosion current density of the Q345 base metal material reflects the high corrosion rate of the material, which is not suitable for service when in direct contact with the atmosphere.

1. INTRODUCTION

Steel structures are widely used in power grids. Some important equipment and facilities, such as transmission lines and transformers, are directly related to the safe and stable operation of power systems and the safe use of electricity by users [1,2]. Because some steel structural components have been used outdoors for a long time, they are extremely susceptible to corrosion from the external environment, and some other components can be affected by a high-voltage electric field. With extended service time, all kinds of equipment and facilities will be corroded and damaged to varying degrees. This corrosion can not only bring great economic losses and energy waste to the power transmission and transformation industry but also hide dangers for safe and stable operation [3]. There are DC electric field environments near substations, and power transmission and transformation equipment adsorbs ions

and dust to a certain extent, which intensifies material corrosion [4]. Chen et al. [5] analyzed the galvanic corrosion, oxygen concentration corrosion, stress corrosion and intergranular corrosion of metal parts in electrical equipment. Chen et al. [6] summarized the causes of rust and corrosion in transmission towers and related protection methods and proposed antiaging coatings. Usually, for different service environments and different parts of power transmission and transformation equipment, an appropriate coating system will be selected as a protective means to prolong the service life of steel. Coating protection can reduce costs by more than half [7]. However, after a period of service, the coating will also fail due to its own aging. Therefore, the mechanism of coating failure needs to be further studied.

To assess the failure mechanism of coating systems, numerous scholars have conducted in-depth research and examinations. Some scholars [8,9,10] have found that the failure of a coating / metal system can be divided into several processes: (1) the coating is wetted by water absorption, and the surface-soluble corrosive medium is dissolved; (2) the internal pressure inside and outside the coating causes the corrosive medium to penetrate from the microdefects, and the generated internal stress forms blisters inside the coating; (3) the corrosive medium reaches the metal matrix, resulting in metal corrosion under the film; and (4) cathodic stripping is caused by metal corrosion. The contact characteristics and interfacial properties of different metal substrates and coatings are different. Leng et al. [11,12,13] studied the defect parts of the coating and believed that the delamination of the coating was affected by the type and concentration of cations in the solution. The smaller the size of cations or the higher their concentration, the faster the delamination rate of the coating. Deflorian et al. [14] showed that when cations diffuse or penetrate into the coating, the cations need to balance the charge due to the existence of anions, so the diffusion rate is increased.

However, there are relatively few reports on the corrosion aging behaviors and electrochemical mechanisms of coating systems of power transmission and transformation equipment in an outdoor atmospheric environment. In this paper, through outdoor exposure tests of a carbon steel coating system on power transmission and transformation equipment in Beijing and Zhengzhou for one year, the aging behavior of each cycle coating and the corrosion characteristics of bare metal are studied. Electrochemical impedance spectroscopy (EIS) and polarization curves were analyzed to explain the corrosion and aging behavior of carbon steel and the coating system of transmission and transformation equipment in a subhumid atmosphere of a northern temperate zone.

2. MATERIALS AND METHODS

2.1. Outdoor exposure tests

The carbon steel coating samples were hung outdoors in Beijing and Zhengzhou, and 3 sampling cycles were set up for 3, 6 and 12 months. The samples exposed outdoors included bare metal and coated carbon steel systems. The material of the coating carbon steel system was Q345 carbon steel, and the sample size was 150×70×2 mm. The surface of the metal substrate was sprayed with an anti-corrosion coating after sandblasting. The anticorrosive coating system was an epoxy primer + fluorocarbon polyurethane topcoat. The thickness of the primer was 80–100 μm, and the thickness of the topcoat

ranged from 100 to 120 μm. To prevent a large amount of rainwater or pollutants from depositing on the surface of the samples, they were tilted at 45°. Sampling tests were carried out after each cycle.

The climate survey results of Beijing and Zhengzhou are as follows:

Beijing: The annual average temperature is 12.5 °C, July is the hottest month, and the monthly average temperature is 26 °C; January is the coldest month, and the monthly average temperature is -4.5 °C. The average rainfall is 483.9 mm, the annual average sunshine time is approximately 2600 hours, and the irradiation amount is bout 5500 MJ/(m^2·a).

Zhengzhou: The annual average temperature is 14.3 °C; July is the hottest month, with a monthly average temperature of 27.3 °C; January is the coldest month, with a monthly average temperature of -0.2 °C. The annual average rainfall is 632 mm. The annual sunshine time is approximately 2400 hours, and the irradiation amount is approximately 4800 MJ/(m^2·a). (Data come from China Weather Network www.weather.com.cn)

Comparing the environment of the two places, the climate types are similar, belonging to the north temperate subhumid atmosphere, and the annual average temperature has little difference. However, comparing the rainfall and sunshine time, Beijing is relatively dryer and the sunshine time is longer. On the whole, there is little difference between the two regions, which are typical subhumid atmospheric environments in the north temperate zone. It is hot and rainy in summer and cold and dry in winter, with a large daily temperature difference and long sunshine duration throughout the year.

2.2. Coating EIS test

To study and evaluate the protective performance of the coating during outdoor service in Beijing and Zhengzhou, the electrochemical impedance method was used. A three-electrode system was adopted. The working electrode was a coated sample connected to the metal matrix, the auxiliary electrode was a platinum electrode, and the reference electrode was a saturated calomel electrode. The test solution was a 3.5% NaCl solution. The exposed area of the sample in the solution is 10 cm^2. The test was carried out at 25 °C. First, the coating was soaked on the test area for a period of time, and the open circuit potential was measured during the soaking process. When the potential value fluctuated less than 10 mV within 15 min, the system was considered to be stable. Then, EIS tests were started, where the scanning frequency range was 10^5 Hz~10^{-2} Hz, the disturbance potential was 20 mV, and 10 test points were set in each order of magnitude. Each group of tests was repeated at least 5 times to ensure the true reliability of the data. Finally, the curve with the low-frequency impedance modulus as the median was taken as the research object. The data were fitted by ZSimpWin software and plotted by Origin software.

2.3 Metal polarization curve test

To characterize the corrosion resistance of metal after coating damage or aging failure, the polarization curve of metal specimens in each cycle was tested. The test also used a three-electrode system, and the working electrode was a bare metal sample that was connected to the polished part. The

test solution of the experiment was also a 3.5% NaCl solution, and it was carried out at 25 °C. First, the open circuit potential was measured for 30 min to ensure the stability of the system, and the potential polarization curve was tested. The setting range of the sweep potential was ±500 mV relative to the open circuit potential, and the sweep rate was 0.5 mV/s. At least 3 different parts were taken for testing. The test results were plotted and fitted by Origin software to obtain the corrosion potential E_{corr} and corrosion current density i_{corr}.

3. RESULTS AND DISCUSSION

3.1 EIS analysis of coatings

Figure 1 and Figure 2 show the electrochemical impedance spectra of the coatings exposed outdoors for different cycles in Beijing and Zhengzhou, respectively. Referring to the principle of corrosion electrochemistry [15], Figure 3 shows the equivalent circuit in the initial aging of the coating used for fitting [16], and the fitting results are shown in Table 1 and Table 2, respectively.

Due to the existence of the dispersion effect, the impedance at the interface between the metal and coating cannot be regarded as an ideal capacitance [17]. The constant phase angle element Q is used to replace the capacitive element, which is defined as:

$$Z = \frac{1}{Y_0}(j\omega)^{-n}$$

where

Z—Impedance of Q

j—Unit imaginary part

ω—Angular frequency

Y_0—Constant

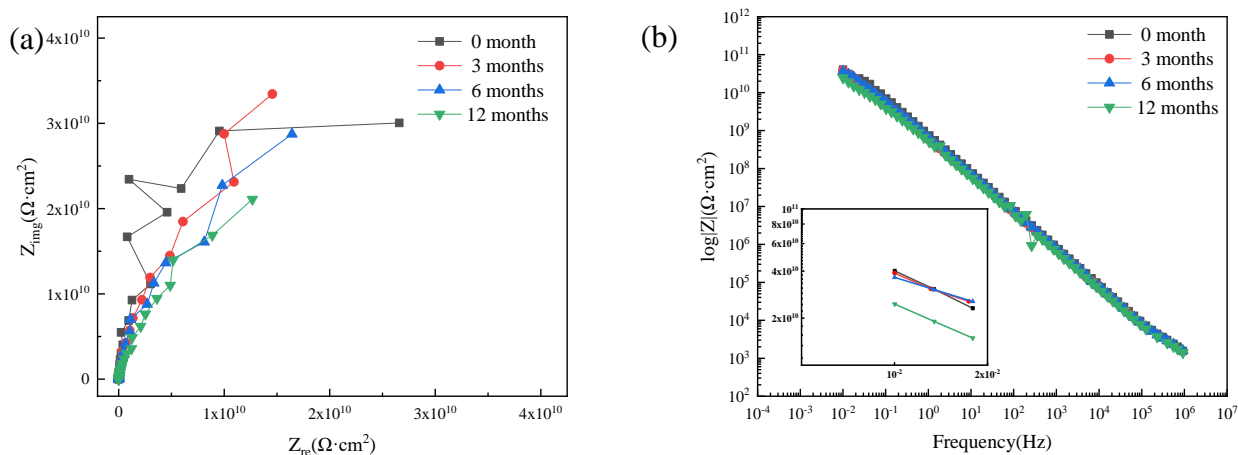n—Dispersion effect index of Q $(0<n<1)$

Figure 1. EIS of the carbon steel coating system at different outdoor exposure times in Beijing: (a) Nyquist plot, (b) Bode plot (Note: this includes the coating samples of the outdoor exposure test for 0, 3, 6 and 9 months.)
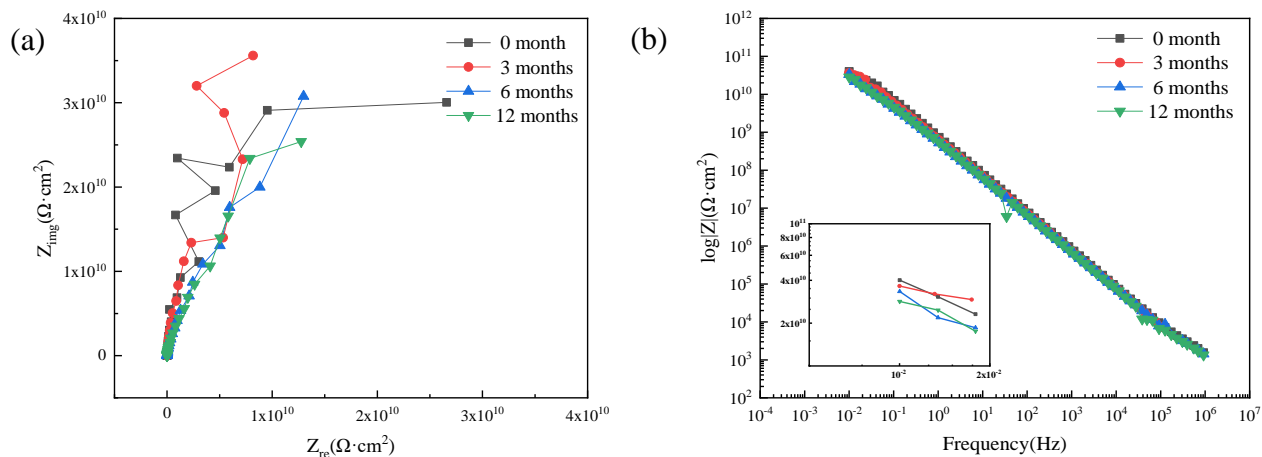
Figure 2. EIS of the carbon steel coating system at different outdoor exposure times in Zhengzhou: (a) Nyquist plot, (b) Bode plot (Note: this includes the coating samples of the outdoor exposure test for 0, 3, 6 and 9 months.)
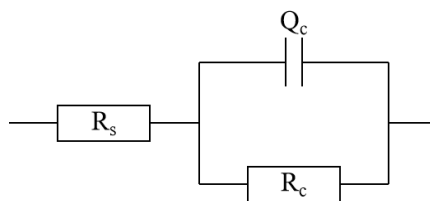

Figure 3. Equivalent Circuit of Coating

Table 1. EIS fitting parameters of the carbon steel coating system at different outdoor exposure times in Beijing (Note: this includes the coating samples of the outdoor exposure test for 0, 3, 6 and 9 months.)

Period	R_s ($\Omega \cdot cm^2$)	Y_0 (F/cm^2)	n	R_c ($\Omega \cdot cm^2$)	$|Z|_{0.01Hz}$ ($\Omega \cdot cm^2$)
0 month	5.303×10^2	7.131×10^{-11}	0.9789	2.446×10^{11}	4.012×10^{10}
3 months	5.128×10^2	8.579×10^{-11}	0.9656	2.550×10^{11}	3.880×10^{10}
6 months	5.138×10^2	8.360×10^{-11}	0.9740	1.837×10^{11}	3.647×10^{10}
12 months	4.405×10^2	1.075×10^{-10}	0.9629	8.536×10^{10}	2.461×10^{10}

Table 2. EIS fitting parameters of the carbon steel coating system at different outdoor exposure times in Zhengzhou (Note: this includes the coating samples of the outdoor exposure test for 0, 3, 6 and 9 months.)

Period	R_s ($\Omega \cdot cm^2$)	Y_0 (F$\cdot cm^{-2}$)	n	R_c ($\Omega \cdot cm^2$)	$|Z|_{0.01Hz}$ ($\Omega \cdot cm^2$)
0 month	5.303×10^2	7.131×10^{-11}	0.9789	2.446×10^{11}	4.012×10^{10}
3 months	1.140×10^3	2.680×10^{-10}	0.9749	1.522×10^{11}	3.650×10^{10}
6 menlths	5.144×10^2	1.079×10^{-11}	0.9513	2.135×10^{11}	3.339×10^{10}
12 months	4.533×10^2	1.030×10^{-10}	0.9599	1.855×10^{11}	2.842×10^{10}

It can be seen from the Nyquist plots in Figure 1(a) and Figure 2(a) that the curves of each period do not form a stable semicircular arc. Under the equivalent circuit in Figure 3, the coating resistance R_c is equivalent to the charge transfer resistance of the system [18] and is the resistance to ionic conduction between the metal matrix and solution. The value of R_c can reflect the difficulty of electrochemical reactions at the matrix interface, but it also decreases with the aging of the coating [16,17,19]. According to the fitting results, R_c is basically $1 \times 10^{11} \sim 2 \times 10^{11}$ $\Omega \cdot cm^2$, which shows that the electrochemical reaction on the metal surface is very difficult. Y_0 can reflect the capacitance characteristics of the coating. Smaller values indicate better capacitance characteristics and lower porosity [18]. The fitting result is basically maintained at approximately 1×10^{-10} $F \cdot cm^{-2}$, reflecting that the coating can maintain good shielding performance after each cycle.

According to the Bode modulus plots in Figure 1(b) and Figure 2(b), the curve of each cycle basically maintains an oblique straight line, which indicates that the coating has good capacitance characteristics and always maintains excellent shielding performance for corrosive media [20]. The coincidence of the curves is better, indicating that the degree of aging is low. For the low-frequency region of the Bode plot, the impedance modulus value reflects the state of the coating and the metal interface. The lower the low-frequency impedance modulus value is, the higher the penetration degree of the corrosive medium or the electrolyte solution into the coating and the higher the aging degree of the coating [21]. According to the statistics of the impedance modulus at 0.01 Hz, it can be seen that the aging degree of the samples in the two regions also changed significantly with increasing of outdoor exposure time.

Comparing the law of curve change between Beijing and Zhengzhou, it can be seen that the coating has obvious changes within one year, the protective performance has decreased, and the low-frequency impedance modulus value reflects that the aging degree of the coating in the two regions is also close.

3.2 Potentiodynamic polarization curves

Figure 4 (a) and (b) show the test results of the polarization curves of bare metal materials in Beijing and Zhengzhou, respectively. The curve fitting results are shown in Table 3 and Table 4.

From the polarization curve and fitting results, it can be seen that the variation law of the polarization curve in each cycle is basically similar in Beijing and Zhengzhou. The corrosion potential E_{corr} of the original sample of the Q345 bare material is the lowest, but E_{corr} also increases with increasing outdoor exposure time. The corrosion potential reflects the thermodynamic stability of the metal surface system. With increasing outdoor exposure time, the higher the E_{corr} of the sample is, the higher the thermodynamic stability of the surface [22].
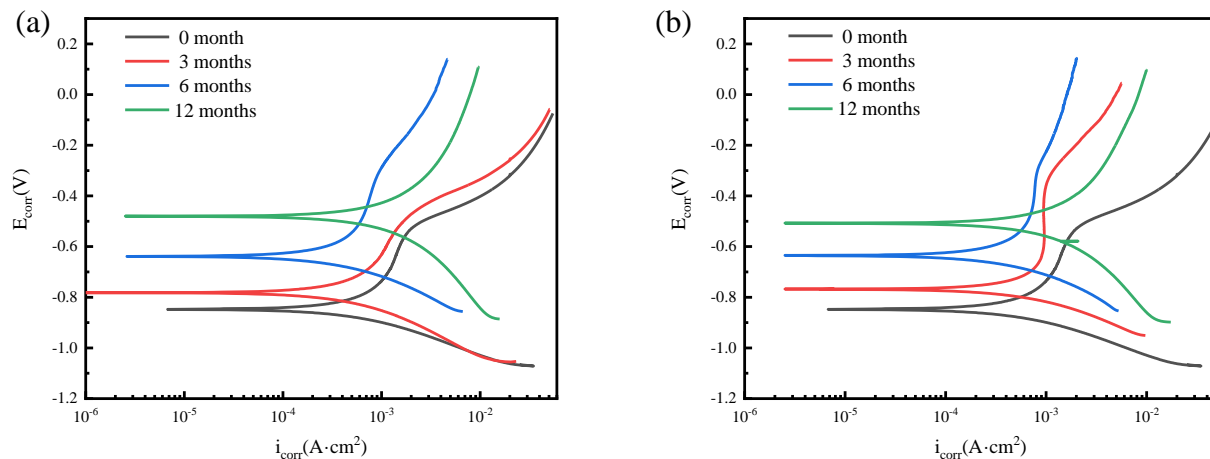
Figure 4. Polarization curves of carbon steel bare metal at different outdoor exposure times in (a) Beijing and (b) Zhengzhou (Note: this includes the carbon bare metal samples of the outdoor exposure test for 0, 3, 6 and 9 months.)

Table 3. Polarization curve fitting parameters of the polarization curves of carbon steel in Beijing

Period	E_{corr} (mV)	i_{corr} (mA·cm^2)	β_a (mV/decade)	β_c (mV/decade)
0 month	-849	0.668	663	198
3 months	-785	0.324	290	141
6 months	-638	0.381	670	207
12 months	-484	1.651	630	442

Table 4. Fitting parameters of the electrochemical polarization curves of carbon steel in Zhengzhou

Period	E_{corr} (mV)	i_{corr} (mA·cm^2)	β_a (mV/decade)	β_c (mV/decade)
0 month	-849	0.668	663	198
3 months	-772	0.484	464	143
6 months	-640	0.392	651	223
12 months	-503	1.547	580	437

This may be due to the continuous corrosion and the formation of corrosion products. The area of the active area in direct contact with the corrosion medium decreases, resulting in an increase in the thermodynamic stability of the system at the macro level. The corrosion current density i_{corr} reflects the corrosion rate of the metal. i_{corr} gradually decreases in the early stage and increases after 6 months. The reason for the decrease in the early stage may be the continuous increase in corrosion products, mainly γ-FeOOH and Fe_3O_4, on the surface, resulting in a gradual decrease in the corrosion rate [23]. When the corrosion products increase to a certain extent, a double rust layer will be formed. With irregular outdoor precipitation and changes in of temperature and humidity during the day and night, the existence of a

double rust layer will keep some electrolyte solution between the rust layers, which will indirectly increase the corrosion rate of the metal.

3.3 Aging analysis of the carbon steel coating system

According to the test of the coating impedance and the polarization curve of the Q345 carbon steel substrate in Beijing and Zhengzhou, the aging law of the coating during outdoor service in the subhumid atmosphere of the northern temperate zone was analyzed. The function of the coating is to isolate the corrosive medium in the atmosphere from the metal matrix and prevent the metal from corroding through physical means. The outdoor exposure test of bare carbon steel also shows that the corrosion rate is relatively fast. If there is no coating protection, the service life will be greatly reduced.

For the aging process of the coating, there is abundant sunshine in the environment, and the influence of ultraviolet rays in the sunlight on the coating cannot be ignored. In the subhumid atmosphere of the northern temperate zone, the annual radiation amount is approximately 5000 MJ/(m^2·a), and a large amount of energy is transmitted in the form of ultraviolet rays. Ultraviolet radiation increases the surface energy of polymer coatings, and some chemical bonds are gradually broken, which may form hydrophilic groups [24,25]; in addition, this may further crosslink the polymer macromolecular chains on the surface and increase the tension degree of the polymer links, thereby increasing the hardness and brittleness of the coating on the macroscopic level [26,27]. Long-term ultraviolet radiation will cause an increasing number of microdefects on the surface of the coating [28].

The increase in defects and the emergence of hydrophilic groups make it easier for the liquid film produced by irregular rainfall and daily temperature and humidity changes in the outdoor environment to remain in the coating surface, pores and defects. Over a long timeframe, the damage will gradually deepen from outside to inside until the coating is completely aged and invalid.

When this process is reflected in EIS, the original new coating can be compared to a very perfect capacitor. The curve in the Nyquist plot is not a semicircular arc but is more similar to a straight line with a larger slope [28]. The point in the low-frequency region is approximately closer to the imaginary part, indicating that the capacitance characteristic is stronger; the Bode modulus curve is a straight line with a negative slope, which also shows the capacitance characteristics of the coating system [29].

After one year of outdoor exposure tests, the change in the electrochemical impedance test results of the coating is small, which is reflected in the decrease in the impedance modulus in the low-frequency region, which generally reflects the strong aging resistance of the coating. Combined with the aging mechanism of the coating, this is mainly due to the defects of the coating after aging, which makes the corrosive medium in the environment invade into the interior of the coating and destroys the characteristics of the perfect capacitance of the coating. The local capacitance characteristics and capacitance values are continuously reduced at the defect site, which is shown in the fitting results as the increase in Y_0 and the decrease in n, where n reflects the smoothness and integrity of the coating surface [30].

As aging progresses, the low-frequency impedance modulus in the Bode plot will continue to decrease until a horizontal line with a slope of 0 appears in the low-frequency band, and the surface

coating becomes a protection method with resistance as the main characteristic. This also shows that the metal substrate has been in communication with the external corrosive medium, and the coating has completely failed [30].

After the coating fails, the test results of the polarization curve of the metal show that at the corrosion rate of Q345 carbon steel, the equipment in service will soon fail. Therefore, in this type of coating system, to ensure the safe operation of the equipment, it is not suitable for service in the open atmosphere, and the integrity and effectiveness of the surface coating must be ensured.

4. CONCLUSION

(1) Under the subhumid atmospheric environment in the north temperate zone, there is little difference between the aging of coatings and the corrosion properties of metals in Beijing and Zhengzhou.

(2) In a 1-year outdoor exposure test, a polarization curve test of bare material Q345 carbon steel shows that the corrosion rate of the material is high, which is not suitable for exposure in the atmosphere, and will soon fail without coating protection.

(3) In a 1-year outdoor exposure test, an electrochemical impedance test of the coating system shows that the coating has good capacitance characteristics, reflecting good protective performance against the metal substrate.

References

1. J. Yang, J. Han, M. Li, F. Li and F. Yang, *Power System Technology*, 34 (2010) 1.
2. Z. Ding, C. Huang, H. Xue, L. Zhu and M. Zhu, *Electric Power Construction*, 6 (2012) 105.
3. Z. Song, J. Guo and J. Guo, *Shanxi Electric Power*, 149 (2008) 7.
4. X. Ren, W. Qian, Y. Zhong, G. Wu, J. Hao and J. Liu, *2019 IEEE 3rd International Electrical and Energy Conference*, (2019) 1649.
5. H. Chen, X. Qiao, F. Tian and Y. Sun, *2020 3rd International Conference on Electron Device and Mechanical Engineering*, (2020) 88.
6. Y. Chen, C. M. Qiang, G. Wang and W. Miao, *Corrosion Science and Protection Technology*, 25 (2013) 508.
7. X. Li, D. Zhang, Z. Liu, Z. Li, C. Du and C. Dong, *Nature*, 527 (2015) 441.
8. M. Morcillo, *Prog. Org. Coat.*, 36 (1999) 137.
9. S. B. Lyon, R. Bingham, D. J. Mills, *Prog. Org. Coat.*, 102 (2016) 2.
10. Fuente, D. Chico, B. Morcillo, *Portugaliae Electrochimica Acta*, 24 (2006) 191.
11. A. Leng, H. Streckel and M. Stratmann, *Corros. Sci.*, 41 (1998) 547.
12. A. Leng, H. Streckel and M. Stratmann, *Corros. Sci.*, 41 (1998) 579.
13. A. Leng, H. Streckel, K. Hofmann and M. Stratmann, *Corros. Sci.*, 41 (1998) 599.
14. F. Deflorian and S. Rossi, *Electrochimica Acta*, 51 (2006) 1736.

15. C. Cao, *The corrosion electrochemistry principle*, Chemical Industry Press, (2004) Beijing, China.
16. Q. Thu, H. Takenouti and S. Touzain, *Electrochimica Acta*, 51 (2006) 2491-2502.
17. E. Akbarinezhad, F. Rezaei and J. Neshati, *Prog. Org. Coat.*, 61 (2008) 45-52.
18. J. Fernandes, A. Nunes, M. Carvalho and T. Diamantino, *Solar Energy Materials and Solar Cells*, 160 (2017) 149-163.
19. T. S. Lopes, T. Lopes, D. Martin, C. Carneiro, J. Machado and A. Mendes, *Prog. Org. Coat.*, 138 (2020) 105365.
20. X. Liu, J. Xiong, Y. Lv and Y. Zuo, *Prog. Org. Coat.*,64 (2009) 497-503.
21. F. Lu, B. Song, P. He, Z. Wang and J. Wang, *RSC Adv.*, 7 (2017) 13742-13748.
22. M. Kim and J. Kim, *Int. J. Electrochem. Sci.*, 10 (2015) 6872-6885.
23. Y. Liu, Z. Wang and Y. Wei, *Int. J. Electrochem. Sci.*, 14 (2019) 1147-1162.
24. M. Irigoyen, P. Bartolomeo, F. Perrin, E. Aragon and J. Vernet, *Polym. Degrad. Stab.*, 74 (2001) 59.
25. L. Valentinelli, J. Vogelsang, H. Ochs and L. Fedrizzi, *Prog. Org. Coat.*, 45 (2002) 405.
26. B. Johnson and R. Mcintyre, *Prog. Org. Coat.*, 27 (1996) 95.
27. A. Ghasemi-Kahrizsangi, J. Neshati, H. Shariatpanahi and E. Akbarinezhad, *Prog. Org. Coat.*, 85 (2005) 199.
28. M. Irigoyen, E. Aragon, F. Perrin and J. Vernet, *Prog. Org. Coat.*, 59 (2007) 259.
29. F. Deflorian, S. Rossi and M. Fedel, *Corros. Sci.*, 50 (2008) 2360.
30. H. Ochs, J. Vogelsang and G. Meyer, *Prog. Org. Coat.*, 46 (2003) 182.